



Article

First Pangenome of *Corynebacterium rouxii*, a Potentially Toxigenic Species of *Corynebacterium diphtheriae* Complex

Fernanda Diniz Prates ^{1,2} , Max Roberto Batista Araújo ¹ , Eduarda Guimarães Sousa ² , Juliana Nunes Ramos ³ , Marcus Vinícius Canário Viana ² , Siomar de Castro Soares ⁴ , Louisy Sanches dos Santos ³ and Vasco Ariston de Carvalho Azevedo ^{2,*}

¹ Operational Technical Nucleus, Microbiology, Hermes Pardini Institute, Vespasiano 33200-000, MG, Brazil; fernandaprates3@hotmail.com (F.D.P.)

² Institute of Biological Sciences, Federal University of Minas Gerais, Belo Horizonte 31270-901, MG, Brazil; eduardaguimaraessousa@gmail.com (E.G.S.)

³ Laboratory of Diphtheria and Corynebacteria of Clinical Relevance, Department of Microbiology, Immunology and Parasitology, Rio de Janeiro State University, Rio de Janeiro 20551-030, RJ, Brazil; louisysanchesuerj@gmail.com (L.S.d.S.)

⁴ Institute of Biological and Natural Sciences, Federal University of Triângulo Mineiro, Uberaba 38025-350, MG, Brazil; siomars@gmail.com

* Correspondence: vascoariston@gmail.com; Tel.: +55-31-3409-2610

Abstract: *Corynebacterium rouxii* is one of the recently described species of the *Corynebacterium diphtheriae* complex. As this species can potentially infect different hosts and harbor the *tox* gene, producing diphtheria toxin, we present its first pangenomic analysis in this work. A total of fifteen genomes deposited in online databases were included. After confirming the taxonomic position of the isolates by genomic taxonomy, the genomes were submitted to genomic plasticity, gene synteny, and pangenome prediction analyses. In addition, virulence and antimicrobial resistance genes were investigated. Finally, epidemiological data were obtained through molecular typing, clustering, and phylogenetic analysis. Our data demonstrated genetic diversity within the species with low synteny. However, the gene content is extensively conserved, and the pangenome is composed of 2606 gene families, of which 1916 are in the core genome and 80 are related to unique genes. Prophages, insertion sequences, and genomic islands were found. A type I-E CRISPR-Cas system was also detected. Besides the *tox* gene, determinants involved in adhesion and iron acquisition and two putative antimicrobial resistance genes were predicted. These findings provide valuable insight about this species' pathogenicity, evolution, and diversity. In the future, our data can contribute to different areas, including vaccinology and epidemiology.

Keywords: *Corynebacterium rouxii*; *Corynebacterium diphtheriae* complex; virulence factors; antimicrobial resistance genes; CRISPR-Cas system; pangenome



Citation: Prates, F.D.; Araújo, M.R.B.; Sousa, E.G.; Ramos, J.N.; Viana, M.V.C.; Soares, S.d.C.; dos Santos, L.S.; Azevedo, V.A.d.C. First Pangenome of *Corynebacterium rouxii*, a Potentially Toxigenic Species of *Corynebacterium diphtheriae* Complex. *Bacteria* **2024**, *3*, 99–117. <https://doi.org/10.3390/bacteria3020007>

Academic Editor: Margaret L. Britz

Received: 3 April 2024

Revised: 12 May 2024

Accepted: 14 May 2024

Published: 16 May 2024



Copyright: © 2024 by the authors. Licensee MDPI, Basel, Switzerland. This article is an open access article distributed under the terms and conditions of the Creative Commons Attribution (CC BY) license (<https://creativecommons.org/licenses/by/4.0/>).

1. Introduction

Corynebacterium comprises a collection of aerobic or facultatively anaerobic, non-acid-fast, non-spore-forming, and irregular rod-shaped microorganisms with a high GC content. The type species is *Corynebacterium diphtheriae*, known as the main etiological agent of diphtheria, a contagious infection that can affect the respiratory tract and skin. The main signs and symptoms result from the action of diphtheria toxin (DT), an exotoxin produced by the microorganism when lysogenized by phages carrying the *tox* gene [1].

Despite advances resulting from universal vaccination programs with the diphtheria toxoid, which drastically reduced the number of cases worldwide, diphtheria is still reported even in immunized individuals [2,3]. In recent years, the number of cases and outbreaks of diphtheria have been reported in several countries, including Brazil, where

diphtheria is endemic, as well as Austria, Belgium, France, Norway, Switzerland, and the United Kingdom [2–6].

Besides *C. diphtheriae*, the closely related species *Corynebacterium belfanti*, *Corynebacterium pseudotuberculosis*, *Corynebacterium rouxii*, *Corynebacterium silvaticum*, and *Corynebacterium ulcerans*, which form the *C. diphtheriae* complex, can also harbor the *tox* gene and produce DT [7–9].

C. rouxii was described in 2020 based on the genomic taxonomy of six atypical maltose-negative strains, isolated from humans and one dog, previously identified as *C. diphtheriae* biovar Belfanti [10]. In this same study, atypical biovar Belfanti strains isolated from cats in the USA [9] were also reclassified as *C. rouxii*. Considering these recent taxonomic reclassifications, some earlier names should be corrected to *C. rouxii*. Until this moment, the latest cases of *C. rouxii* infection have been reported in the USA [11], Germany [12], Spain [13], and Brazil [14].

In the present work, we present the first pangenomic analysis of *C. rouxii*, contributing to the identification of potential virulence factors and genes related to antimicrobial resistance and a better understanding of the pathogenic potential and evolution of this recently described species of *Corynebacterium*.

2. Materials and Methods

2.1. Genome Data Retrieval from Public Database

For comparative analysis of *C. rouxii*, we used the National Center of Biotechnology Information (NCBI—<https://www.ncbi.nlm.nih.gov/>, accessed on 12 January 2024) and the European Nucleotide Archive (ENA—<https://www.ebi.ac.uk/ena/browser/home>, accessed on 14 January 2024) databases to retrieve the genomic sequences. A total of 15 genomes of *C. rouxii* were downloaded in nucleotide FASTA format from NCBI and in text-based format FASTQ from ENA. The quality analysis of the sequences was performed using FastQC (<https://github.com/s-andrews/FastQC>, accessed on 21 January 2024). All genomes downloaded from ENA were assembled using Unicycler v.0.5.0 (<https://github.com/rrwick/Unicycler>, accessed on 21 January 2024) and contigs with less than 200 bp were trimmed. To evaluate the guanine and cytosine (GC) content, size, and fragmentation of the genomes, we used QUAST (<https://github.com/ablab/quast>, accessed on 22 January 2024). The completeness and contamination levels were estimated using CheckM2 (<https://github.com/chklovski/CheckM2>, accessed on 22 January 2024) and the completeness of rRNA genes was estimated using Barnapp (<https://github.com/tseemann/barnap>, accessed on 22 January 2024). Information about the sequences is provided in Table 1. All genomes were annotated using Prokka v.1.14.6 (<https://github.com/tseemann/prokka>, accessed on 22 January 2024) [15].

Table 1. Information about the fifteen genomic sequences of *C. rouxii* strains.

Strain	Database	Status	Size (Mb)	CDS	GC%	BioSample	Country	Host	Reference Article
FRC0190 ^T	NCBI	Complete	2,451,019	2366	53	SAMEA5992727	France	Human	[10]
21395	NCBI	Draft	2,357,570	2238	53	SAMN35995151	Brazil	Dog	Current study
58111	NCBI	Draft	2,354,960	2241	53	SAMN35995239	Brazil	Dog	Current study
70862	NCBI	Draft	2,399,341	2447	53	SAMN34030355	Brazil	Cat	[14]
70863	NCBI	Draft	2,380,082	2397	53	SAMN34030356	Brazil	Cat	[14]
FRC0071	ENA	Reads	2,400,198	2321	53	SAMEA5992726	France	Human	[10]
FRC0284	ENA	Reads	2,381,258	2302	53	SAMEA5992728	France	Human	[10]
FRC0297	ENA	Reads	2,272,976	2165	53	SAMEA5992729	France	Human	[10]
FRC0412	ENA	Reads	2,385,950	2322	53	SAMEA5992730	France	Dog	[10]
FRC0527	ENA	Reads	2,390,401	2315	53	SAMEA5992731	France	Human	[10]
PC0230	ENA	Reads	2,430,051	2362	53	SAMN13343876	USA	Cat	[11]
PC0231	ENA	Reads	2,430,200	2362	53	SAMN13343877	USA	Cat	[11]
PC0226	ENA	Reads	2,430,047	2359	53	SAMN13343873	USA	Cat	[11]
PC0229	ENA	Reads	2,429,572	2364	53	SAMN13343875	USA	Cat	[11]
CS30	ENA	Reads	2,345,163	2260	53	SAMEA7617347	Spain	Human	[13]

2.2. Taxonomy, Typing, and Phylogeny

The taxonomy of the strains was determined using TYGS (<https://tygs.dsmz.de/>, accessed on 3 February 2024). Sequence type (ST) was determined in silico considering seven housekeeping genes, *atpA*, *dnaE*, *dnaK*, *fusA*, *leuA*, *odhA*, and *rpoB*, according to the MLST scheme defined in PubMLST [16] and using the FastMLST script (<https://github.com/EnzoAndree/FastMLST>, accessed on 3 February). Average Nucleotide Identity (ANI) values among the *C. rouxii* strains were calculated using PyANI v.0.2.12 (<https://github.com/widdowquinn/pyani>, accessed on 6 February 2024). DNA-DNA hybridization (DDH) was determined in silico for the genomes using the Type (Strain) Genome Server (<https://tygs.dsmz.de>, accessed on 6 February 2024). Genomes were clustered using PopPUNK v.2.6.0 [17], and the network was visualized using Cytoscape v.3.10.1 [18].

The phylogenetic tree based on the MLST scheme was built using OrthoFinder pipeline v.2.5.5 (<https://github.com/davidemms/OrthoFinder>, accessed on 22 March 2024) with the MAFFT algorithm [19] for protein sequence alignment and FastTree (<http://www.microbesonline.org/fasttree/>, accessed on 22 March 2024) for tree inference (parameter “-M msa”). The tree was visualized using iTOL v.6 (<https://itol.embl.de/>, accessed 22 March 2024). For the wgMLSTtree, whole genome sequences were uploaded into PGAdg-builder (<http://wgmlstdb.imst.nsysu.edu.tw/>, accessed on 24 March 2024), and the core genes with default parameters (90% coverage and 90% identity) were chosen [20].

2.3. Prediction of Mobile Genetic Elements, CRISPR-Cas Systems, and Genomic Islands

PlasmidFinder v.2.1.6 was used for the in silico detection of plasmids [21], and IntegronFinder v.2.0 was used for identifying and analyzing integrons across the genomes [22]. The prophage sequences were identified and annotated with Phage Search Tool Enhanced Release (PHASTER) [23]. Average Nucleotide Identity (ANI) values were calculated among the predicted intact prophages and their closest phages using PyANI v.0.2.12. Prophage regions with ANI identity values > 95.0% were aligned using tblastx [24], and compared and visualized using the Easyfig application [25]. Moreover, the Insertion Sequences (IS) were identified using ISEScan [26]. CRISPRCasFinder v.1.1.2 was used to analyze the presence of Clustered Regularly Interspaced Short Palindromic Repeats (CRISPRs) and Cas proteins [27]. In our analyses, we included only CRISPR arrays with evidence levels equal to 3 or 4 [27], and the type of CRISPR-Cas cassette was determined following the previously described nomenclature and classification [28]. Spacer sequences were analyzed for their identity in the CRISPRTarget database [29]. Spacer hits were selected from the CRISPRTarget with a cut-off Identity Cover (IC) score above 0.80 [30].

The prediction of putative genomic islands was performed using GIPSY v.1.1.2 [31], with *Corynebacterium glutamicum* ATCC 13,032 (GenBank accession number GCA_000011325.1) as a reference for non-pathogenic closely related organism [32]. Circular genome map comparisons were built using BRIG (Blast Ring Image Generator) software v.0.95 [33], including reference positions for antimicrobial resistance genes, virulence factors, and genomic islands. Functional annotation was performed with EggNOG-mapper v.2.1.11 [34] to explore the genes in the islands.

2.4. Gene Synteny

The software Mauve v.20150226 and the progressive Mauve algorithm were used to construct multiple genome alignments, which provided information about evolutionary events such as rearrangement and inversion [35].

2.5. Virulence Factors and Antimicrobial Resistance Genes

VFanalyzer was implemented to screen potential virulence factors in all *C. rouxii* strains using the VFDB (Virulence Factor Database) database [36]. Additionally, we used PanViTa v.1.1.3 [37] to search for antimicrobial resistance genes and virulence genes using the CARD (Comprehensive Antibiotic Resistance Database) and VFDB databases, respectively, for more accurate results. The phylogeny of the *tox* gene from *C. rouxii* and other species from

the *C. diphtheriae* complex was inferred from the maximum likelihood method based on the Tamura 3-parameter model using Mega v6 and bootstrap values with 1000 replicates [38].

2.6. Pangenome Development and Functional Annotation

Pangenomic analysis was performed with the Bacterial Pan Genome Analysis pipeline (BPGA) v.1.3, using the following options to configure the analysis: 50% identity cut-off and USEARCH as a default-clustering tool [39]. According to Clusters of Orthologous Groups (COG), the coding sequences (CDS) of the core genome, accessory, and unique gene subsets were aligned and classified based on the functional categories [40]. EggNOG-mapper v.2.1.11 was used to perform the functional annotation according to orthologous genes [34]. DIAMOND v2.0.14.152 (<https://github.com/bbuchfink/diamond/releases>, accessed on 10 March 2024) was chosen for the initial sequence-mapping step by eggNOG-mapper. The most suitable matching of sequence mapping was classified according to its taxonomy. Finally, it was categorized and annotated according to gene ontology (GO) [41], KEGG pathways [42], and COG functional categories [43], which have several categories.

3. Results

3.1. Taxonomy, Typing, and Phylogeny

All strains were classified as *C. rouxii* by TYGS (Supplementary Table S1). Six different STs were identified: 74 (USA, cat), 181 (France, human), 537 (France, human; Spain, human), 538 (France, dog), 899 (Brazil, cat), and 918 (Brazil, dog) (Supplementary Table S2). The ANI values among strains ranged from 0.98 to 1.0 (Supplementary Figure S1). The strains formed five clusters. Four of them had the same host and country: Cluster 1 (USA, cat), Cluster 2 (France, human), Cluster 4 (Brazil, dog), and Cluster 5 (France, dog). Cluster 3 had isolates from cats in Brazil, humans in France, and humans in Spain (Supplementary Figure S2).

The phylogenetic tree based on the MLST scheme showed two main clades. The first clade contained only the American strains (PC0226, PC0229, PC0230, and PC0231), while the other clade contained the Brazilian, French, and Spanish strains, composed of two main subclades. In the first one, only the French strains were clustered, as FRC0190^T, FRC0284, FRC0071, and FRC0527 had more phylogenetic proximity than FRC0412. In the other subclade, we could observe that the Brazilian strains clustered and separated from the French and Spanish strains. However, 70862 and 70863 demonstrated more phylogenetic proximity with the latter than 21395 and 58111 (Figure 1). No phylogenetic difference was observed when constructing the wgMLSTtree (Supplementary Figure S3).

3.2. Prediction of Mobile Genetic Elements, CRISPR-Cas Systems, and Genomic Islands

The analysis performed with PlasmidFinder v.2.1.6 did not detect plasmids in the genomes of any strain, and IntegronFinder v.2.0 did not identify any integrons in the genomes.

Using PHASTER, we predicted 57 prophage regions, which were classified into intact ($n = 3$), incomplete ($n = 46$), and questionable ($n = 8$). Detailed information is presented in Supplementary Table S3. A total of 25 different phages were found. The most common phage was *Corynebacterium* Poushou, present in 12 strains, followed by *Gordonia* GMA5 and *Rhodococcus* Sleepyhead, present in seven and five strains, respectively. Intact prophages were found in the genomes of the 58111, PC0226, and PC0231 strains. After the analysis of ANI values considering all matching regions between intact prophage regions of *C. rouxii* and the most common phages, we realized that the ANI value between PC0226 and PC0231 was 1.0, and the ANI value between PC0226 and *Escherichia* phage lato was 0.99, as well as between PC0231 and *Escherichia* phage lato. On the other hand, 58,111 prophages did not present identity with any of the closest phages detected by PHASTER (Supplementary Figure S4).

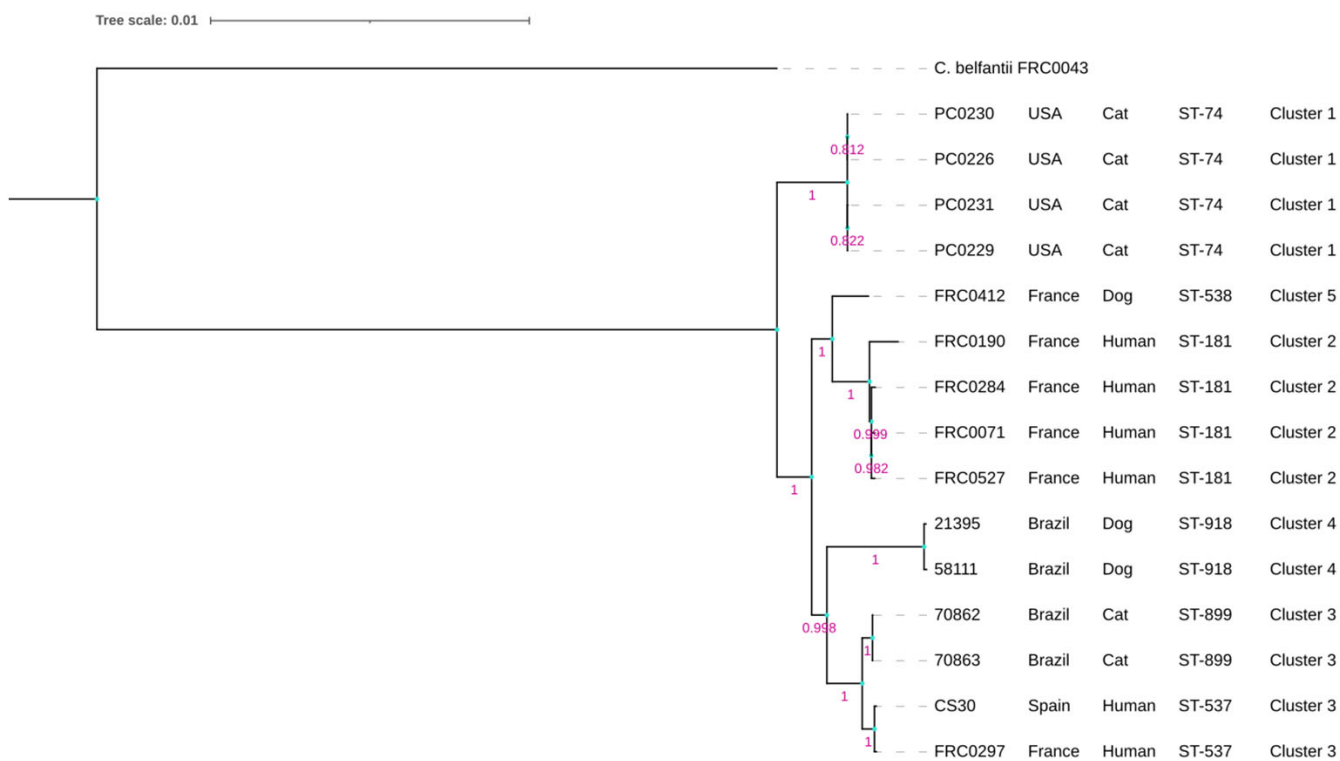


Figure 1. Phylogenetic tree based on MLST scheme showing the relationship between all genomes of *C. rouxii* strains. The tree was built using OrthoFinder pipeline v.2.5.5 and distance was inferred based on neighbor joining (p-distance). Bootstrap values with 1000 replicates. The scale bar indicates 0.01% divergence. *C. belfanti* FRC0043^T was used as an outgroup.

The image generated using the Easyfig application shows the identity between the intact prophages from the PC0226 and PC0231 strains and the similar products of the genes present in these regions, such as C protein, gpA protein, minor and major spike proteins, capsid, DNA packaging, and external scaffolding proteins (Figure 2A). The gpA protein of the PC0231 prophage was found to be translocated and 1179 bases were deleted when compared with the same protein in the PC0226 prophage. On the other hand, the intact prophage from the 58111 strain, more significant than the others, presented the following products in its region: recombination, tail fiber, tail assembly, capsid decoration, phage portal major proteins, besides terminals, head maturation protease, methyltransferase, and some hypothetical proteins (Figure 2B).

The prediction of insertion sequences carried out in ISEScan revealed the following numbers of elements in the genome of each strain: FRC0190^T (IS = 33); FRC0071 and FRC0412 (IS = 32); 21395 and 58111 (IS = 30); FRC0284 (IS = 29); 70862 and 70863 (IS = 28); FRC0527 (IS = 27); PC0226 (IS = 26); PC0230, PC0231, and CS30 (IS = 25); and FRC0297 and PC0229 (IS = 24). The IS were grouped into seven families (IS110, IS21, IS256, IS3, IS30, IS5, and ISL3). Information about the number of IS families in each strain is in Supplementary Table S4.

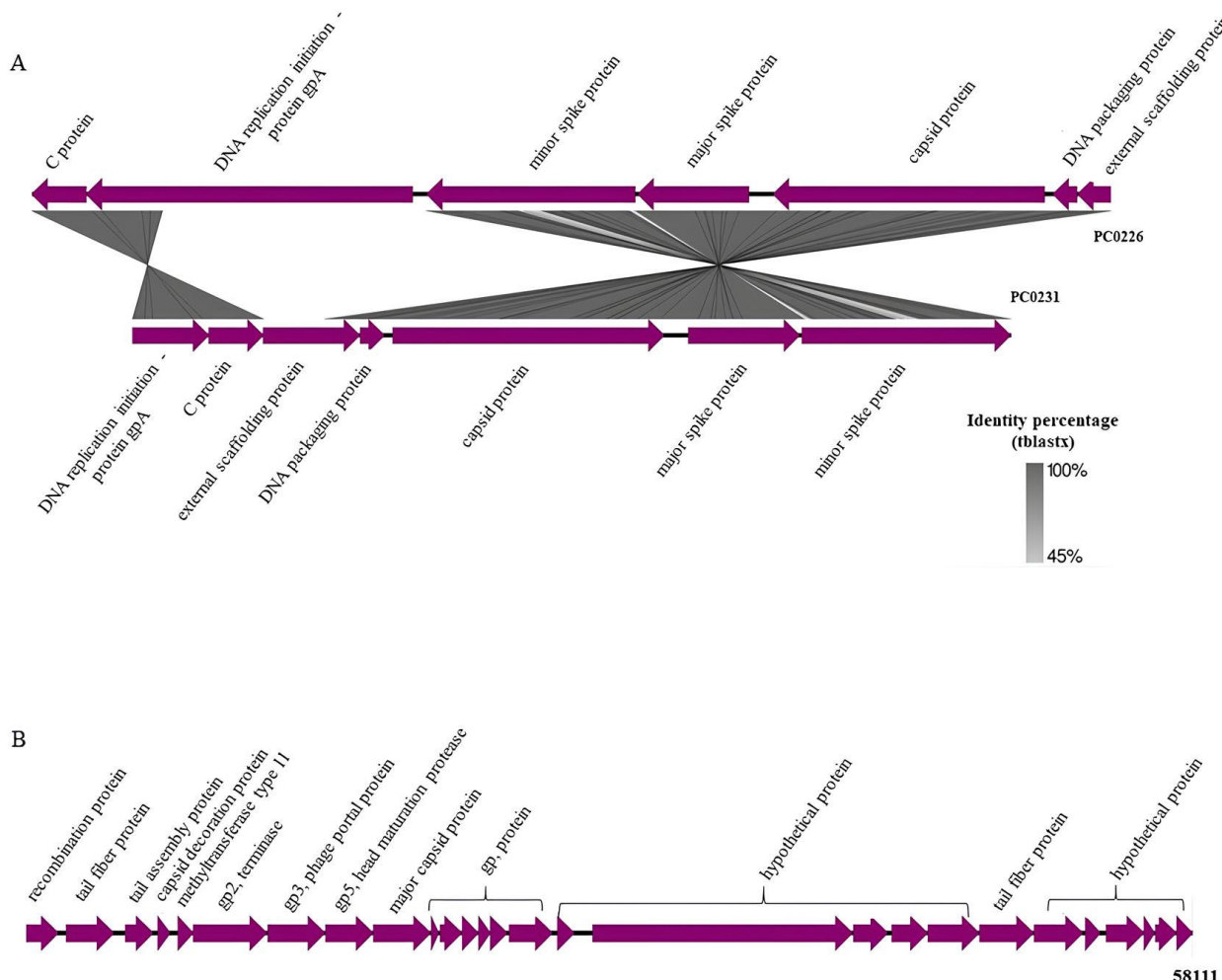


Figure 2. Intact prophage regions. (A) Comparison between *C. rouxii* PC0226 and PC0231 strains using Easyfig, and the main products present in each region. The BLAST identity scale is shown on the right with matches ranging from 45% to 100% identity. (B) Products of genes present in *C. rouxii* 58,111 strain using Easyfig.

The CRISPRCasFinder server identified the type I-E CRISPR-Cas system, lacking the *cas3* gene in all strains. A total of 13 regions related to CRISPR were detected with an evidence level equal to 4 (Supplementary Table S5). FRC0284 and CS30 were the unique strains that did not present a CRISPR system with high precision for spacer repetition and similarity. Analysis of the spacer diversity among all of the CRISPR arrays found 292 spacer sequences, in which the FRC0412 strain carried the largest number of them (70 spacers). The other strains presented the following numbers of sequences: FRC0190^T (33 spacers); 21395, 58111, and FRC0071 (29 spacers); FRC0527 (22 spacers); FRC0297 (17 spacers); 70862 and 70863 (16 spacers); PC0226, PC0229, and PC0230 (8 spacers); and PC0231 (7 spacers). All spacers with values above 80% identity from the CRISPRTarget server are presented in Supplementary Table S5.

Figure 3 shows the similarity between FRC0190^T and the other *C. rouxii* genomes, providing comparative genomic plasticity results. The GC content was 53.81%. Considering only strong predictions, it was possible to check the presence of nine genomic islands (GI 1–GI 9). We found several genes involved in biological processes: transport (ABC and serine transporter), adherence (*spaD*-type pili), uptake and translocation of the essential macronutrient phosphorus (phosphate transporter), iron uptake, and the siderophore biosynthesis system (*ciuABCD*).

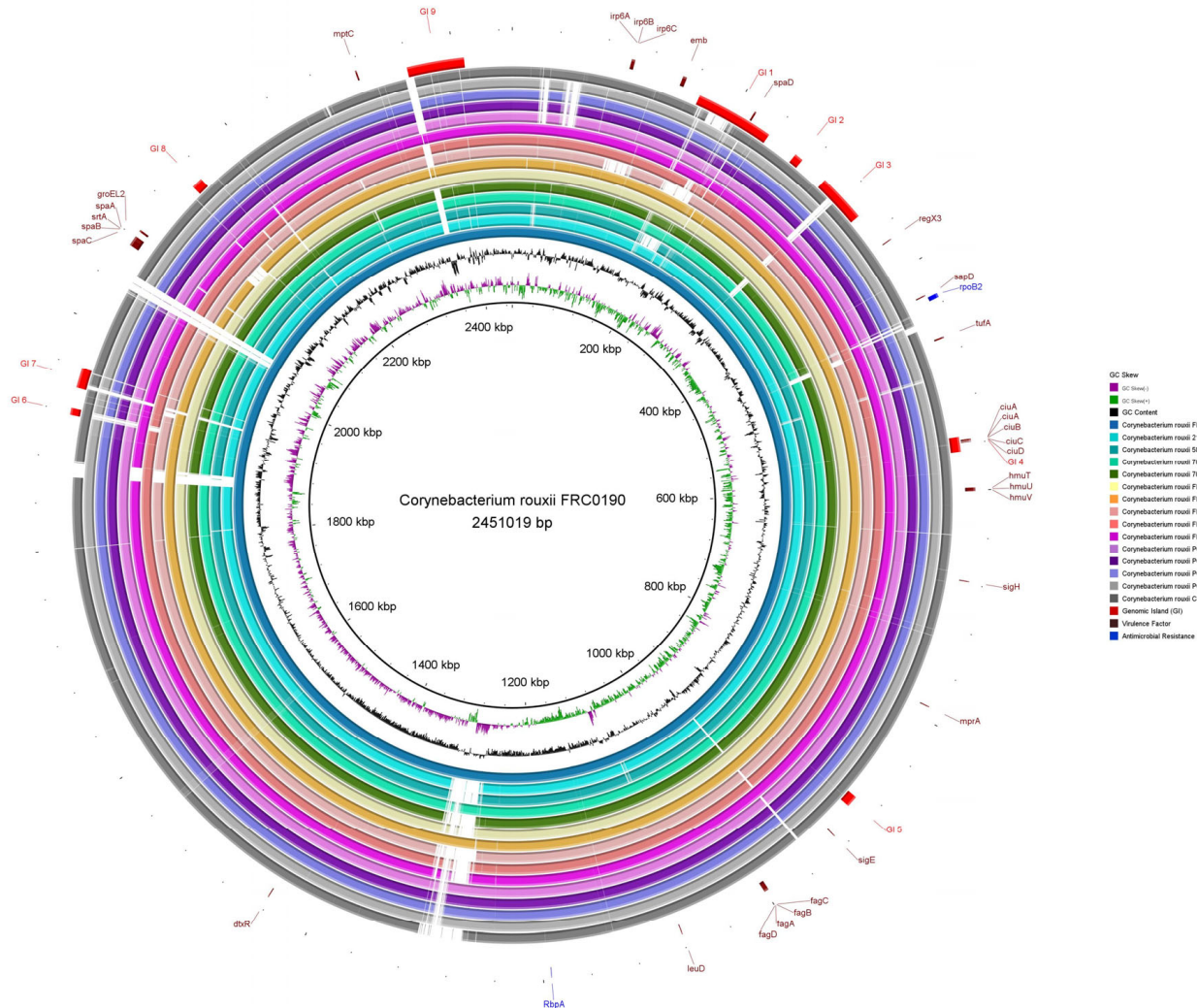


Figure 3. Circular comparative map of all complete genomes of *C. rouxii* using BRIG. As a reference genome, we used *C. rouxii* FRC0190^T [10], which is represented in this map in the central position with the first three rings showing its size, GC content, and GC skew. Each outer ring represents the complete genome of one specific strain of *C. rouxii*. The genomic islands are represented by arcs in red color, the virulence factors by the maroon default, and antimicrobial resistance genes by the blue default.

3.3. Gene Synteny

After multiple alignments between FRC0190^T and the other *C. rouxii* genomes, it was possible to visualize that, although the gene content was conserved inside the blocks, the strains presented rearrangements over large parts of the genome, including inversions and translocations. Some deletion blocks, mainly at the ends of the genomes, were also visible. These results are presented in Supplementary Figure S5.

3.4. Virulence Factors and Antimicrobial Resistance Genes

As observed in Figure 4, compared to VFDB reference *C. rouxii* FRC0190^T, the *tox* gene was identified in four strains (PC0226, PC0229, PC0230, and PC0231), and the sequences of this gene differed from that found in *C. diphtheriae*, *C. pseudotuberculosis*, *C. silvaticum*, and *C. ulcerans* (Figure 5). Additionally, as shown in Figure 4, in all strains, except the FRC0527 strain, a complete pilus cluster (*spaABC*) was detected, and in the FRC0190^T, 70862, 70863, FRC0297, and CS30 strains, an incomplete *spaDEF* (only *spaD*) was detected. In all strains, genes involved in the ABC transporter, ABC-type heme transporter, and Ci

iron uptake systems were detected. All strains, except 21395, 58111, 70862, and 70863, also presented the *ciuD* gene. FRC0297 was the unique strain in which no gene involved in a siderophore-dependent iron uptake system was detected. Some genes, such as *dtxR*, *embC*, and *mptC*, were also predicted in all strains, including *rpoB2* and *rbaP*.

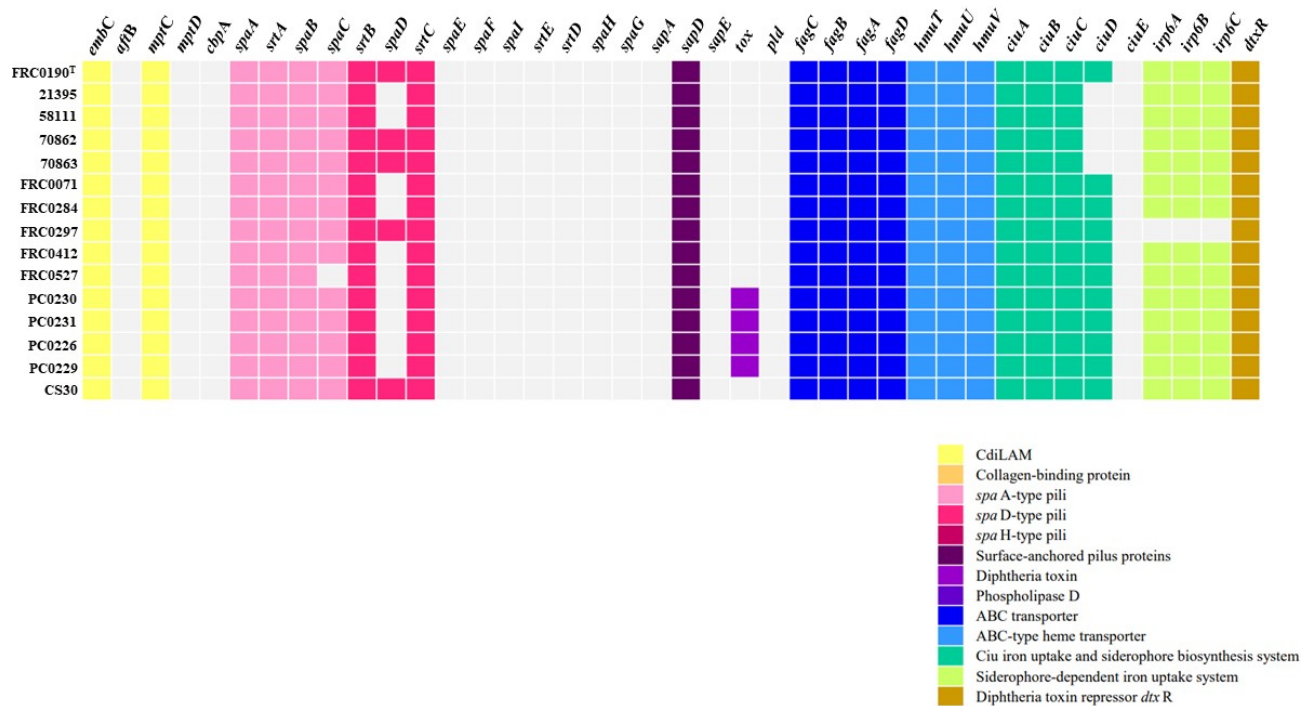


Figure 4. Distribution of virulence factors in each *C. rouxii* genomic sequence. For better understanding, virulence factors are grouped into functional classes, represented by a specific color according to the legend.

3.5. Pangenome Development and Functional Annotation

For the pan-genome analysis of *C. rouxii*, we predicted 2606 gene families (Figure 6A), including 1916 in the core genome (73.5%), 610 related to accessory genes (23.4%), and 80 related to unique genes (3.1%). The distribution of accessory and unique genes in each strain is shown in Figure 6B. The α value was less than 1, approximately 0.95 ($\alpha = 1 - 0.05$).

The distribution of COG functional classifications in the pangenome of the *C. rouxii* strains showed the prevalence of several categories according to the organization of genes into core, accessory, and unique groups (Figure 7). The main COG subcategories in the core genome were amino acid transport and metabolism (10.7%); translation, ribosomal structure, and biogenesis (8.5%); transcription (7.0%); replication, recombination, and repair (6.7%); and inorganic ion transport and metabolism (6.5%). Accessory genes were mainly related to replication, recombination, and repair (17.6%); inorganic ion transport and metabolism (9.9%); transcription (7.8%); amino acid transport and metabolism (5.2%); and cell wall/membrane/envelope biogenesis (5.2%). On the other hand, unique genes were mainly involved in replication, recombination, and repair (34.0%); defense mechanisms (16.5%); carbohydrate transport and metabolism (16.5%); and cell wall/membrane/envelope biogenesis (16.5%). A total of 204 genes presented function unknown, comprising 128 genes (6.7%) in the core genome and 76 genes (12.4%) in accessory genes (Figure 7). The functional annotation of KEGG is shown in Figure 8.

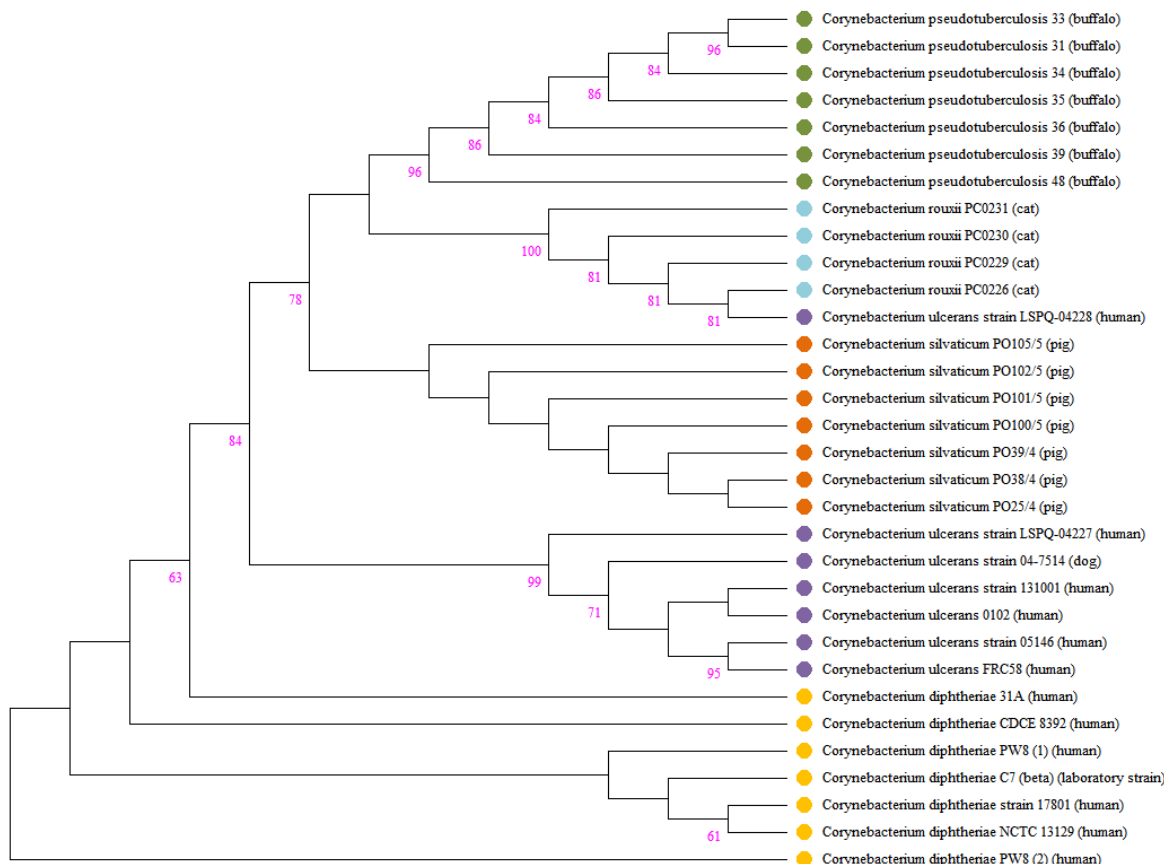


Figure 5. Phylogeny of *tox* gene from *C. rouxii*, *C. diphtheriae*, *C. pseudotuberculosis*, *C. silvaticum*, and *C. ulcerans*. The tree was inferred using the maximum likelihood method based on the Tamura 3-parameter model using Mega v6. Bootstrap values with 1000 replicates.

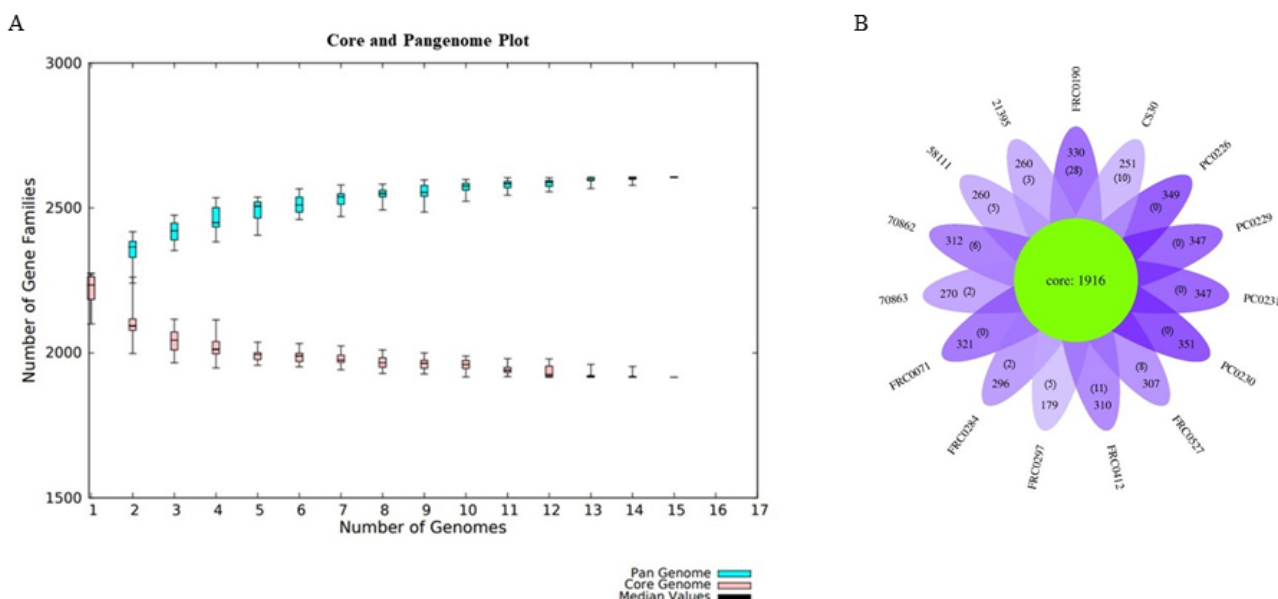


Figure 6. Pangenome development. **(A)** Pangenome growth curve with Heap's law using the BPGA pipeline. The plot shows the number of gene families in the pangenome (blue) and in the core genome (pink). **(B)** Flower plot diagram of the *C. rouxii* pangenome generated by R script, showing the core gene families (green). The number of accessory genes for each strain are indicated on each petal and the number of unique genes is in the parentheses.

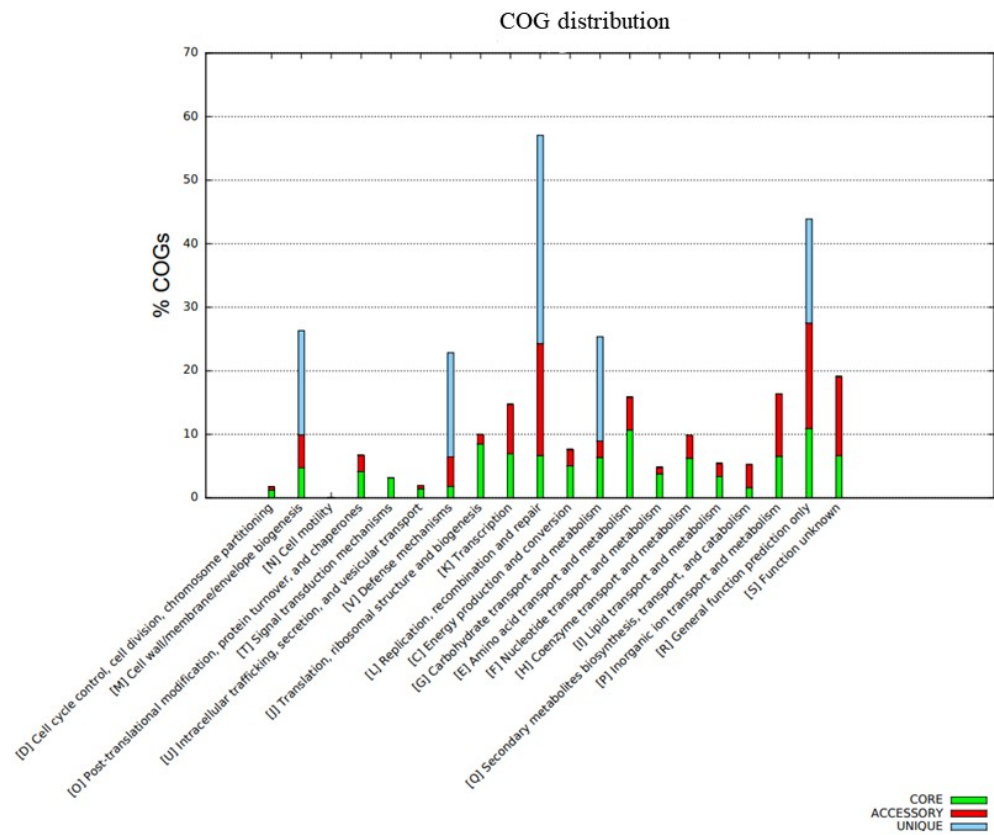


Figure 7. Function annotation using the BPGA pipeline in which the bar graph represents the COG classifications of the pangenome. The core genome is represented by the green color, the accessory genome is represented by the red color, and unique genes are represented by the blue color.

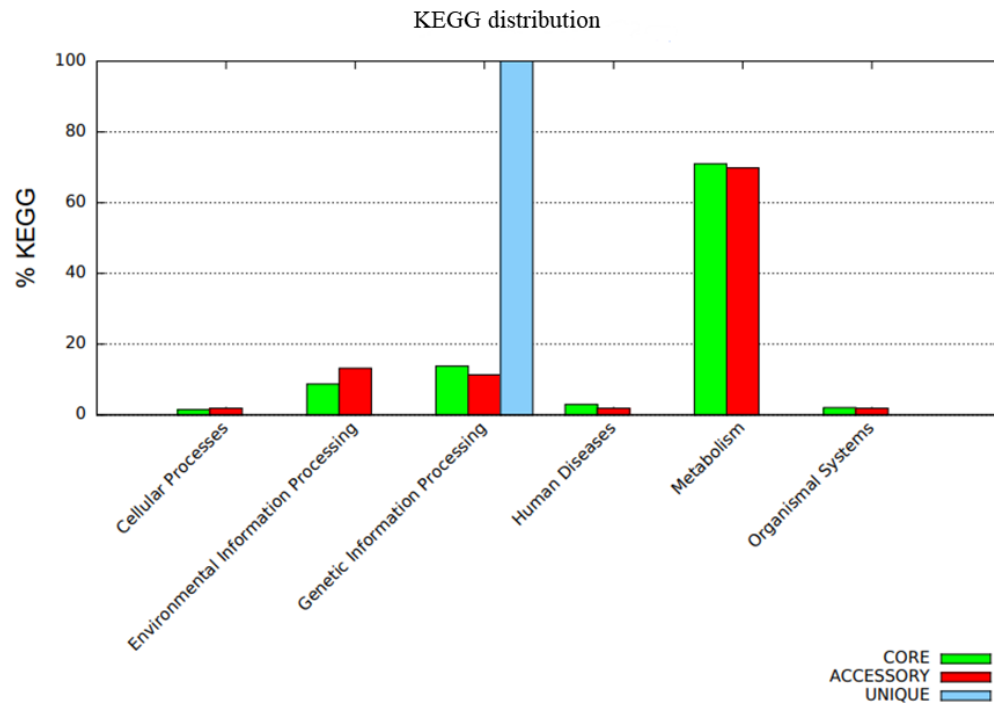


Figure 8. Functional annotation using the BPGA pipeline in which the bar graph represents the KEGG classifications of the pangenome. The core genome is represented by the green color, the accessory genome is represented by the red color, and unique genes are represented by the blue color.

4. Discussion

In recent years, taxonomic analysis based on the genome of *C. diphtheriae* strains led to the description of the novel species *C. belfanti* and *C. rouxii* [8,10]. Until now, *C. rouxii* has been found to cause different infections in humans, dogs, and cats [9–14]. Although the potential to infect other host species and to produce DT is a matter of concern, few studies in the literature have focused on the virulence factors, mechanisms of antimicrobial resistance, and metabolic pathways of this species. In this sense, we performed the first pangenomic analysis of this species, providing valuable insight into its pathogenicity, evolution, and diversity.

Additionally, to ensure the quality of data, the 15 strains for which their genomes were deposited in the NCBI and ENA databases were first confirmed based on dDDH and ANI values, which were consistent with values above the proposed cut-off points for species limit, corroborating identification of the strains as *C. rouxii*. Considering the need to obtain epidemiological data on this emerging pathogen, we also submitted the genomes to molecular typing, clustering, and phylogenetic analysis.

MLST has been widely used in different countries for genotyping circulating *C. diphtheriae* and *C. ulcerans* strains and in investigations of diphtheria outbreaks [44–46]. With the description of novel species of the *C. diphtheriae* complex, the MLST scheme has also been applied to typing the isolates of these species. In our analyses, six STs could be attributed to the *C. rouxii* strains. More than one ST was attributed to isolates from each host species (human, cat, and dog), showing a certain genetic diversity. No ST was found simultaneously in animal and human isolates. Moreover, ST-537 was found in two European countries, France and Spain, which alerts for a possible circulation of this ST in these countries.

Classical MLST is typically based on sequences from only seven housekeeping genes; hence, this approach does not fully exploit core and accessory genomic variation. It cannot further discriminate genetically related isolates within STs [17,47]. Thus, we also performed a population analysis and clustering with PopPUNK software. In addition, we constructed a phylogenetic tree based on wgMLST to investigate the genetic diversity between our isolates and compare MLST and PopPUNK results. All of the analyses showed the genetic diversity of *C. rouxii*. Although MLST and PopPUNK provided similar results, the phylogenetic analysis revealed the little greater discriminatory power and typeability of MLST. Further studies, including more isolates, should be performed to confirm this divergence. As expected, wgMLST was the optimal method for molecular subtyping *C. rouxii* isolates. Considering that whole genome sequencing is not accessible in many countries, MLST appears to be a satisfactory alternative tool for epidemiological studies involving this species.

It is known that bacterial adaptive evolution relies on the diversity of gene repertoires of the species, which can be affected through a variety of processes, including horizontal gene transfer (HGT). In addition to gene acquisition, HGT can result in events of rearrangement and deletions, leading to remarkable changes in the genome over relatively short periods. HGT is one of the main processes responsible for acquiring virulence factors and antibiotic resistance, and it may change the pathogenic profile of bacterial species [48–50]. Thus, the 15 genomes used in this study were analyzed regarding the occurrence of gene duplication, rearrangements, and deletions and the presence of mobile elements, including insertion sequences and genomic islands. Verifying several rearrangement events, including inversions, translocations, and deletions, was possible.

It is known that plasmids can be responsible for conferring a selective advantage to bacteria, such as antimicrobial resistance or virulence genes [51]. This can drastically change the prevalence of bacterial clones that are more virulent or multidrug-resistant, facilitating their rapid evolution and adaptation abilities [52]. Although plasmids were not detected in any *C. rouxii* strain in the present work, they were previously reported in *C. diphtheriae* strains, including a 14.4 kb plasmid, pNG2, which, despite not having any important function in toxicity, can encode erythromycin resistance [53,54]. More recently, a multi-resistance plasmid (pLRPD) carrying genes related to penicillin (*pbp2m*,

blaB), sulfamethoxazole (*sul1*), trimethoprim (*dfrA16*), erythromycin (*erm*), and tetracycline resistance (*tetA* family *tet(Z)*-like) was also predicted in *C. diphtheriae* [55].

Moreover, our analyses did not identify any integron in the *C. rouxii* genomes. Integrons are genetic elements that capture and incorporate gene cassettes by site-specific recombination, converting them into functional genes. They are composed of genes for integrase (*int*) and an adjacent recombination site (*attI*). Gene cassettes are not necessarily part of an integron but can be incorporated [56]. The same result was obtained in a previous study evaluating the antimicrobial resistance in *C. pseudotuberculosis*, and no integron was identified [57]. Differently, a recent study detected in *C. diphtheriae* an integron flanked by two insertion sequences (IS6100 and IS1628), comprising genes involved in the resistance to trimethoprim (*dfrA16*), sulfamethoxazole (*sul1*), chloramphenicol (*cmlA*), and aminoglycosides (*aad1*) [58]. A class 1 integron mobilized by IS6100 and carrying some of these genes (*dfrA16*, *sul1*) had already been identified in the genome of a *C. diphtheriae* strain [59]. Interestingly, in the pLRPD of *C. diphtheriae*, some of the antimicrobial resistance genes (*dfrA16*, *sul1*) were found in a truncated class 1 integron [55].

The genome of *C. diphtheriae* complex strains has been characterized by presenting several prophages that are an essential source of genomic plasticity in these species [60]. We identified many incomplete prophage sequences, probably due to the draft or reads sequence status of the genome data retrieved from a public database. On the other hand, we predicted two intact prophages in the 58111, PC0226, and PC0231 strains. The GC content of these prophage sequences was less than the average GC content of 53.0% of *C. rouxii* genomes, except for the 58111 strain.

The *Corynebacterium* phage phi673 (GenBank accession number NC042354), predicted in the 58111 strain, belongs to the *Siphoviridae* family, and was first found as a lytic phage in *C. glutamicum* ATCC 13,032 [61]. The prophage Enterolato (*Escherichia* phage phiX174; GenBank accession number J02482.1), found in the PC0226 and PC0231 strains, belongs to the *Microviridae* family and has a long history of use in several molecular applications [62]. It is commonly found infecting *Escherichia coli* but was also previously reported in ESBL-producing *Klebsiella pneumoniae* isolates. Since our analyses did not show the presence of prophage-encoding resistance and virulence genes, it seems that they are not acting as vectors for disseminating these genes within our strains.

Insertion sequences (IS) are simple and small mobile genetic elements found in most bacterial genomes. A particular bacterial genome can present different types of IS in a wide range of copy numbers. They can move within the genome and be horizontally transferred as part of other mobile elements, such as phages and plasmids, and they can affect the genome structure and gene expression [63–65]. Presently, seven IS families were found in *C. rouxii* genomes (IS110, IS21, IS256, IS3, IS30, IS5 and ISL3). Among those, IS3, one of the largest IS families widely distributed in nature [66], had the highest number of copies in the *C. rouxii* strains. All IS families in our strains were reported previously in *Corynebacterium striatum* isolates [63,66]. In this species, IS110, IS30, IS21, and especially IS3 and IS256 families were associated with antimicrobial resistance [63,66]. The association of IS families with antimicrobial resistance was also verified for other *Corynebacterium* species, including *C. diphtheriae* (IS3) and *Corynebacterium jeikeium* (IS3 and IS256) [66].

Genomic islands are part of the flexible bacterial gene pool that harbors genes derived from mobile elements. They often carry gene clusters with specific functions that can provide a selective advantage to the microorganism. For instance, some genomic islands encode iron-uptake systems, while others carry genes encoding antimicrobial resistance or virulence factors [49]. We investigated the presence and composition of genomic islands in the *C. rouxii* strains. In the nine genomic islands predicted, several genes were found, including those encoding phage integrases and transposases, in addition to genes involved in acquiring and transporting nutrients and adherence. However, no gene related to antimicrobial resistance was found. These results suggest that genomic islands in *C. rouxii*, to date, can contribute to establishing and disseminating this bacterial species in the environment or a host. Still, they are not related to antimicrobial resistance.

CRISPR-Cas is an essential adaptive immune system that helps bacteria and archaea cells not to be infected by phages, viruses, and other foreign genetic elements [67]. This system comprises a CRISPR cluster containing an array of short, direct repeats interspersed with spacer sequences and CRISPR-associated genes (*cas*) [68]. In this study, we found the type I-E CRISPR-Cas system in all strains. CRISPR-Cas systems, especially type I-E, have been reported in *Corynebacterium* species, including those belonging to the *C. diphtheriae* complex. In *C. diphtheriae* strains, besides type I-E CRISPR-Cas, types II and III have already been detected and reported [69]. Using the CRISPRTarget server, the spacer sequences of the strains matched most frequently with corynebacterial (*C. diphtheriae* and *C. ulcerans*), *Rhodococcus* phages, and *Corynebacterium* phage BFK20, present in the pathogenicity island of *C. pseudotuberculosis* isolated from buffalo [70]. Some spacers also matched with other phages found in *Staphylococcus* phage phi7401PVL and *Pseudomonas mendocina* S5.2.

The production of DT after lysogenization by corynebacteriophages that harbor the *tox* gene has already been verified in the species *C. diphtheriae*, *C. ulcerans*, and *C. pseudotuberculosis* [71]. For the other species forming the *C. diphtheriae* complex, there is a consideration that they are potentially toxigenic. To date, no study has demonstrated the presence of the *tox* gene in *C. rouxii* genomes. In our study, we detected the presence of this important gene in four strains (PC0226, PC0229, PC0230, and PC0231), all isolated from animal hosts. The sequence of the *tox* gene was similar in all isolates and differed from that found in *C. diphtheriae*, *C. pseudotuberculosis*, *C. silvaticum*, and *C. ulcerans*. In agreement with a previous study, the *tox* genes isolated from *C. diphtheriae* strains had more phylogenetic proximity with those isolated from *C. ulcerans* [70]. In contrast, in our research, the *tox* genes isolated from *C. rouxii* had more phylogenetic proximity with *C. pseudotuberculosis* and *C. silvaticum*. Notification of potentially toxigenic corynebacteria in animals is not mandatory in most countries; thus, epidemiological data are scarce [72]. However, the presence of the *tox* gene in these species, which are already isolated from humans and animals, may advise about the risk of dissemination of diphtheria.

In the present study, we detected several virulence factors for which their importance has already been demonstrated in previous studies with *C. diphtheriae* and other species. The *embC* and *mptC* genes were identified in all genomes and are related to CdiLAM, which is responsible for forming the characteristic cell envelope in *C. diphtheriae* strains [73]. The gene cluster *spaABC* was detected in all strains, encoding the pili SpaA, which is relevant in the adherence to pharyngeal epithelial cells [74]. The surface-anchored pilus protein *spaD*, involved in adherence, was found in only the FRC0190^T, 70862, 70863, FRC0297, and CS30 strains.

Several systems have been related to iron acquisition in *C. diphtheriae* and related species, including the *fagABC* operon, which is associated with the *fagD* gene [75], the *irp6* operon (*irp6ABC*) [76], and the *ciu* gene cluster, formed by the genes *ciuA*, *ciuB*, *ciuC*, *ciuD*, and *ciuE* [77]. Our data revealed the presence of the *fagABC* operon in all *C. rouxii* strains. The *irp6* operon was not detected in the FRC0297 genome, *ciuD* in the Brazilian strains 21395, 58111, 70862, and 70863, as well as *ciuE*, which was absent in all strains. The absence of these genes may reduce siderophore production and iron uptake.

The iron acquisition from hemin by *C. diphtheriae* requires the ABC-type hemin transporter, HmuTUV, and three hemin-binding proteins (HtaA, HtaB, and HtaC) [78,79]. Unlike previously observations for *C. diphtheriae* [80], in the present study, only the *hmuTUV* cluster was detected entirely in all genomes, suggesting a decreased ability to use hemin as the sole iron source. We detected the *dtxR* gene in all strains, which encodes DtxR, a protein involved in the regulation of DT expression and the synthesis and production of siderophore, besides regulating some other promoters [81]. In addition, DtxR and iron regulate a complex network of genes involved in iron metabolism, including the operon *irp6* and the *ciu* gene cluster [82].

As presented in Figure 3, the genes *rhpA* and *rpoB2*, previously associated with rifampin resistance [55,83–86], were predicted in all genomes. However, additional studies are needed to demonstrate how this resistance occurs in *Corynebacterium* species.

Across the 15 genomes, we identified a pangenome composed of 2606 gene families, of which 1916 were in the core genome, 610 were in the accessory genome, and 80 were related to unique genes. When $\alpha < 1.0$, the pangenome is considered open, which means its size will continuously increase when adding new genomes. In contrast, when $\alpha > 1$, the pangenome is considered closed, meaning that no substantial number of extra genes can be added to the pangenome [87,88]. Our analysis found an alpha value less than 1 (0.95), indicating an open pangenome near to being closed as genes are added. Moreover, there was considerable variation in the number of unique genes, where some strains had more genes, being more variable than others. For example, FRC0190^T had 28 unique genes, while PC0226, PC0229, PC0230, and PC0231 did not have any exclusive genes. It is important to emphasize that the number of genomes in this study was not large, and the composition of the pangenome can change as more genomes are sequenced. Since the first description of the *C. rouxii* strain in 2020, a relatively small number of genomes of this species has been sequenced thus far compared to other related ones belonging to the *C. diphtheriae* complex. So, when comparing the *C. rouxii* and *C. silvaticum* pangenesomes, we noticed that they had similar alpha values, in which some studies have shown values between 0.95 and 0.97 for the latter species [84,89]. Moreover, core genome and singleton analyses agreed with this clonal-like behavior in other complex species. They can also be inferred from pangenome data, in which *C. pseudotuberculosis*, *C. ulcerans*, and *C. diphtheriae* had alpha values of 0.89, 0.81, and 0.69, with pangenesomes composed of 54%, 40%, and 34% core genes families, respectively [89–91].

The distribution of COG showed a high percentage of genes related to replication, recombination, repair, transcription, and amino acid transport and metabolism in the core and accessory genomes of the *C. rouxii* pangenome. This finding was similar to the results reported for the *C. silvaticum* and *C. ulcerans* core genomes [91]. However, regarding the accessory genome in *C. ulcerans*, most genes were involved in translation, ribosomal structure, and biogenesis; lipid and inorganic ion transport and metabolism; and post-translational modification, protein turnover, and chaperones. Most of the differences were found when the *C. rouxii* and *C. diphtheriae* core genomes were compared, mainly because the latter was composed of genes related to the cell wall, membrane, and envelope biogenesis; carbohydrate transport and metabolism; and nucleotide transport and metabolism [92]. Regarding the accessory genome in *C. diphtheriae*, genes were mainly involved in transporting and metabolizing carbohydrates, lipids, and inorganic ions [93].

These findings are relevant for future studies focusing on the search for resistance and virulence genes. They contribute to different areas, including vaccinology and epidemiology. However, they should be corroborated through in vitro and in vivo experimentation.

Supplementary Materials: The following supporting information can be downloaded at: <https://www.mdpi.com/article/10.3390/bacteria3020007/s1>; Table S1: DDH in silico results obtained by the Type Strain Genome Server for *C. rouxii* strains compared to the closest related type strain; Table S2: Information about the Multilocus Sequence Typing for *C. rouxii* strains; Table S3: Information about the prophage regions found in the *C. rouxii* genomes; Table S4: Number of predicted IS families in each *C. rouxii* strain; Table S5: Hits found to spacer sequences in the CRISPRTarget databases; Figure S1: Heatmap representing the ANI percentage nucleotide identity of all matching regions between *C. rouxii* genomes using PyANI v.0.2.12.; Figure S2: Clusters of *C. rouxii* strain genomes generated using PopPUNK v.2.6.0; Figure S3: The wgMLST tree based on genomes from *C. rouxii* strains using PGADB-builder; Figure S4: Heatmap representing the ANI percentage nucleotide identity of all matching regions between intact prophage regions of *C. rouxii* and the most common phages using PyANI v.0.2.12; Figure S5: Gene synteny analysis using the software Mauve.

Author Contributions: Study design, analysis and interpretation of data, and article writing: F.D.P. Study design and acquisition of data: M.R.B.A. Assembling of genomes and annotation: E.G.S. Analysis and interpretation of data: J.N.R. and M.V.C.V. Critical appraisal and article review: S.d.C.S. and L.S.d.S. Conception and design of the study, acquisition of data, analysis, and interpretation of data: V.A.d.C.A. All authors reviewed the manuscript. All authors have read and agreed to the published version of the manuscript.

Funding: This research was funded by Fundação de Amparo à Pesquisa do Estado do Rio de Janeiro (E-26/202.088/2020) and by Coordenação de Aperfeiçoamento de Pessoal de Nível Superior (88887.830701/2023-00).

Institutional Review Board Statement: Not applicable.

Informed Consent Statement: Not applicable.

Data Availability Statement: Genome sequences are available in the NCBI and ENA database according to BioSample numbers shown in Table 1.

Conflicts of Interest: The authors declare no conflicts of interest.

References

- Sharma, N.C.; Efstratiou, A.; Mokrousov, I.; Mutreja, A.; Das, B.; Ramamurthy, T. Diphtheria. *Nat. Rev. Dis. Primers* **2019**, *81*, 1–18. [[CrossRef](#)] [[PubMed](#)]
- Batista Araújo, M.R.; Bernardes Sousa, M.Á.; Seabra, L.F.; Caldeira, L.A.; Faria, C.D.; Bokermann, S.; Sant’Anna, L.O.; Dos Santos, L.S.; Mattos-Guaraldi, A.L. Cutaneous infection by non-diphtheria-toxin producing and penicillin-resistant *Corynebacterium diphtheriae* strain in a patient with diabetes mellitus. *Access Microbiol.* **2021**, *3*, 1–5. [[CrossRef](#)] [[PubMed](#)]
- Araújo, M.R.B.; Ramos, J.N.; de Oliveira Sant’Anna, L.; Bokermann, S.; Santos, M.B.N.; Mattos-Guaraldi, A.L.; Azevedo, V.; Prates, F.D.; Rodrigues, D.L.N.; Aburjaile, F.F.; et al. Phenotypic and molecular characterization and complete genome sequence of a *Corynebacterium diphtheriae* strain isolated from cutaneous infection in an immunized individual. *Braz. J. Microbiol.* **2023**, *54*, 1325–1334. [[CrossRef](#)] [[PubMed](#)]
- Santos, L.S.; Sant’Anna, L.O.; Ramos, J.N.; Ladeira, E.M.; Stavracakis-Peixoto, R.; Borges, L.L.G.; Santos, C.S.; Napoleão, F.; Camello, T.C.F.; Pereira, G.A. Diphtheria outbreak in Maranhão, Brazil: Microbiological, clinical and epidemiological aspects. *Epidemiol. Infect.* **2015**, *143*, 791–798. [[CrossRef](#)] [[PubMed](#)]
- Badenschier, F.; Berger, A.; Dangel, A.; Sprenger, A.; Hobmaier, B.; Sievers, C.; Prins, H.; Dorre, A.; Wagner-Wiening, C.; Kulper-Schiek, W.; et al. Outbreak of imported diphtheria with *Corynebacterium diphtheriae* among migrants arriving in Germany, 2022. *Eurosurveillance* **2022**, *27*, 2200849. [[CrossRef](#)] [[PubMed](#)]
- Wagner, K.S.; White, J.M.; Crowcroft, N.S.; De Martin, S.; Mann, G.; Efstratiou, A. Diphtheria in the United Kingdom, 1986–2008: The increasing role of *Corynebacterium ulcerans*. *Epidemiol. Infect.* **2010**, *138*, 1519–1530. [[CrossRef](#)] [[PubMed](#)]
- Dangel, A.; Berger, A.; Rau, J.; Eisenberg, T.; Kämpfer, P.; Margos, G.; Contzen, M.; Busse, H.J.; Konrad, R.; Peters, M.; et al. *Corynebacterium silvaticum* sp. nov., a unique group of NTTB corynebacteria in wild boar and roe deer. *Int. J. Syst. Evol. Microbiol.* **2020**, *70*, 3614–3624. [[CrossRef](#)] [[PubMed](#)]
- Dazas, M.; Badell, E.; Carmi-Leroy, A.; Criscuolo, A.; Brisse, S. Taxonomic status of *Corynebacterium diphtheriae* biovar Belfanti and proposal of *Corynebacterium belfantii* sp. nov. *Int. J. Syst. Evol. Microbiol.* **2018**, *68*, 3826–3831. [[CrossRef](#)] [[PubMed](#)]
- Hall, A.J.; Cassiday, P.K.; Bernard, K.A.; Bolt, F.; Steigerwalt, A.G.; Bixler, D.; Pawloski, L.C.; Whitney, A.M.; Iwaki, M.; Baldwin, A.; et al. Novel *Corynebacterium diphtheriae* in Domestic Cats. *Emerg. Infect. Dis.* **2010**, *16*, 688–691. [[CrossRef](#)] [[PubMed](#)]
- Badell, E.; Hennart, M.; Rodrigues, C.; Passet, V.; Dazas, M.; Panunzi, L.; Bouchez, V.; Carmi-Leroy, A.; Toubiana, J.; Brisse, S. *Corynebacterium rouxii* sp. nov., a novel member of the diphtheriae species complex. *Res. Microbiol.* **2020**, *171*, 122–127. [[CrossRef](#)]
- Tyler, R.; Rincon, L.; Weigand, M.R.; Xiaoli, L.; Acosta, A.M.; Kurien, D.; Ju, H.; Lingsweiler, S.; Prot, E.Y. Toxigenic *Corynebacterium diphtheriae* Infection in Cat, Texas, USA. *Emerg. Infect. Dis.* **2022**, *28*, 1686–1688. [[CrossRef](#)] [[PubMed](#)]
- Schlez, K.; Eisenberg, T.; Rau, J.; Dubielzig, S.; Kornmayer, M.; Wolf, G.; Berger, A.; Dangel, A.; Hoffmann, C.; Ewers, C.; et al. *Corynebacterium rouxii*, a recently described member of the C. diphtheriae group isolated from three dogs with ulcerative skin lesions. *Antonie Van Leeuwenhoek* **2021**, *114*, 1361–1371. [[CrossRef](#)] [[PubMed](#)]
- Hoefer, A.; Pampaka, D.; Herrera-León, S.; Peiró, S.; Varona, S.; López-Perea, N.; Masacalles, J.; Herrera-León, L. Molecular and Epidemiological Characterization of Toxigenic and Nontoxigenic *Corynebacterium diphtheriae*, *Corynebacterium belfantii*, *Corynebacterium rouxii*, and *Corynebacterium ulcerans* Isolates Identified in Spain from 2014 to 2019. *J. Clin. Microbiol.* **2021**, *59*, 1–15. [[CrossRef](#)]
- Ramos, J.N.; Araújo, M.R.B.; Baio, P.V.P.; Sant’Anna, L.O.; Veras, J.F.C.; Vieira, É.M.D.; Sousa, M.A.B.; Camargo, C.H.; Sacchi, C.T.; Campos, K.R.; et al. Molecular characterization and phylogenetic analysis of the first *Corynebacterium rouxii* strains isolated in Brazil: A recent member of *Corynebacterium diphtheriae* complex. *BMC Genom. Data* **2023**, *24*, 65. [[CrossRef](#)]
- Seemann, T. Prokka: Rapid prokaryotic genome annotation. *Bioinformatics* **2014**, *30*, 2068–2069. [[CrossRef](#)] [[PubMed](#)]
- Guerrero-Araya, E.; Muñoz, M.; Rodríguez, C.; Paredes-Sabja, D. FastMLST: A Multi-core Tool for Multilocus Sequence Typing of Draft Genome Assemblies. *Bioinform. Biol. Insights* **2021**, *15*, 117793222110592. [[CrossRef](#)] [[PubMed](#)]
- Lees, J.A.; Harris, S.R.; Tonkin-Hill, G.; Gladstone, R.A.; Lo, S.W.; Weiser, J.N.; Corander, J.; Bentley, S.D.; Croucher, N.J. Fast and flexible bacterial genomic epidemiology with PopPUNK. *Genome Res.* **2019**, *29*, 304–316. [[CrossRef](#)] [[PubMed](#)]
- Shannon, P.; Markiel, A.; Ozier, O.; Baliga, N.S.; Wang, J.T.; Ramage, D.; Amin, N.; Schwikowski, B.; Ideker, T. Cytoscape: A Software Environment for Integrated Models of Biomolecular Interaction Networks. *Genome Res.* **2003**, *13*, 2498–2504. [[CrossRef](#)] [[PubMed](#)]

19. Katoh, K. MAFFT: A novel method for rapid multiple sequence alignment based on fast Fourier transform. *Nucleic Acids Res.* **2002**, *30*, 3059–3066. [CrossRef] [PubMed]
20. Liu, Y.-Y.; Chiou, C.-S.; Chen, C.-C. PGAdb-builder: A web service tool for creating pan-genome allele database for molecular fine typing. *Sci. Rep.* **2016**, *6*, 36213. [CrossRef] [PubMed]
21. Carattoli, A.; Zankari, E.; García-Fernández, A.; Voldby Larsen, M.; Lund, O.; Villa, L.; Aarestrup, F.M.; Hasman, H. In Silico Detection and Typing of Plasmids using PlasmidFinder and Plasmid Multilocus Sequence Typing. *Antimicrob. Agents Chemother.* **2014**, *58*, 3895–3903. [CrossRef] [PubMed]
22. Néron, B.; Littner, E.; Haudiquet, M.; Perrin, A.; Cury, J.; Rocha, E. IntegratorFinder 2.0: Identification and Analysis of Integrins across Bacteria, with a Focus on Antibiotic Resistance in Klebsiella. *Microorganisms* **2022**, *10*, 700. [CrossRef] [PubMed]
23. Arndt, D.; Grant, J.R.; Marcu, A.; Sajed, T.; Pon, A.; Liang, Y.; Wishart, D.S. PHASTER: A better, faster version of the PHAST phage search tool. *Nucleic Acids Res.* **2016**, *44*, W16–W21. [CrossRef] [PubMed]
24. Johnson, M.; Zaretskaya, I.; Raytselis, Y.; Merezhuk, Y.; McGinnis, S.; Madden, T.L. NCBI BLAST: A better web interface. *Nucleic Acids Res.* **2008**, *36*, W5–W9. [CrossRef] [PubMed]
25. Sullivan, M.J.; Petty, N.K.; Beatson, S.A. Easyfig: A genome comparison visualizer. *Bioinformatics* **2011**, *27*, 1009–1010. [CrossRef] [PubMed]
26. Xie, Z.; Tang, H. ISEScan: Automated identification of insertion sequence elements in prokaryotic genomes. *Bioinformatics* **2017**, *33*, 3340–3347. [CrossRef] [PubMed]
27. Couvin, D.; Bernheim, A.; Toffano-Nioche, C.; Touchon, M.; Michalik, J.; Néron, B.; Rocha, E.P.C.; Vergnaud, G.; Gautheret, D.; Pourcel, C. CRISPRCasFinder, an update of CRISRFinder, includes a portable version, enhanced performance and integrates search for Cas proteins. *Nucleic Acids Res.* **2018**, *46*, W246–W251. [CrossRef]
28. Makarova, K.S.; Koonin, E.V. Annotation and Classification of CRISPR-Cas Systems. In *CRISPR. Methods in Molecular Biology*; Lundgren, M., Charpentier, E., Fineran, P., Eds.; Humana Press: New York, NY, USA; Springer: Berlin/Heidelberg, Germany, 2015. [CrossRef]
29. Biswas, A.; Gagnon, J.N.; Brouns, S.J.J.; Fineran, P.C.; Brown, C.M. CRISPRTarget. *RNA Biol.* **2013**, *10*, 817–827. [CrossRef] [PubMed]
30. Sangal, V.; Fineran, P.C.; Hoskisson, P.A. Novel configurations of type I and II CRISPR-Cas systems in *Corynebacterium diphtheriae*. *Microbiology* **2013**, *159 Pt 10*, 2118–2126. [CrossRef]
31. Soares, S.C.; Geyik, H.; Ramos, R.T.J.; de Sá, P.H.C.G.; Barbosa, E.G.V.; Baumbach, J.; Figueiredo, H.C.P.; Miyoshi, A.; Tauch, A.; Silva, A.; et al. GIPSY: Genomic island prediction software. *J. Biotechnol.* **2016**, *232*, 2–11. [CrossRef] [PubMed]
32. Vertès, A.A.; Inui, M.; Yukawa, H. Postgenomic Approaches to Using *Corynebacteria* as Biocatalysts. *Annu. Rev. Microbiol.* **2012**, *66*, 521–550. [CrossRef] [PubMed]
33. Alikhan, N.-F.; Petty, N.K.; Ben Zakour, N.L.; Beatson, S.A. BLAST Ring Image Generator (BRIG): Simple prokaryote genome comparisons. *BMC Genom.* **2011**, *12*, 402. [CrossRef] [PubMed]
34. Cantalapiedra, C.P.; Hernández-Plaza, A.; Letunic, I.; Bork, P.; Huerta-Cepas, J. eggNOG-mapper v2: Functional Annotation, Orthology Assignments, and Domain Prediction at the Metagenomic Scale. *Mol. Biol. Evol.* **2021**, *38*, 5825–5829. [CrossRef] [PubMed]
35. Darling, A.C.E.; Mau, B.; Blattner, F.R.; Perna, N.T. Mauve: Multiple Alignment of Conserved Genomic Sequence with Rearrangements. *Genome Res.* **2004**, *14*, 1394–1403. [CrossRef] [PubMed]
36. Liu, B.; Zheng, D.; Zhou, S.; Chen, L.; Yang, J. VFDB 2022: A general classification scheme for bacterial virulence factors. *Nucleic Acids Res.* **2022**, *50*, D912–D917. [CrossRef] [PubMed]
37. Rodrigues, D.L.N.; Ariute, J.C.; Rodrigues da Costa, F.M.; Benko-Iseppon, A.M.; Barh, D.; Azevedo, V.; Aburjaile, F. PanViTa: Pan Virulence and resistance analysis. *Front. Bioinform.* **2023**, *3*, 1070406. [CrossRef] [PubMed]
38. Tamura, K.; Stecher, G.; Peterson, D.; Filipski, A.; Kumar, S. MEGA6: Molecular Evolutionary Genetics Analysis Version 6.0. *Mol. Biol. Evol.* **2013**, *30*, 2725–2729. [CrossRef] [PubMed]
39. Chaudhari, N.M.; Gupta, V.K.; Dutta, C. BPGA- an ultra-fast pan-genome analysis pipeline. *Sci. Rep.* **2016**, *6*, 24373. [CrossRef] [PubMed]
40. Galperin, M.Y.; Wolf, Y.I.; Makarova, K.S.; Vera Alvarez, R.; Landsman, D.; Koonin, E.V. COG database update: Focus on microbial diversity, model organisms, and widespread pathogens. *Nucleic Acids Res.* **2021**, *49*, D274–D281. [CrossRef] [PubMed]
41. The Gene Ontology Consortium. Gene Ontology Consortium: Going forward. *Nucleic Acids Res.* **2015**, *43*, D1049–D1056. [CrossRef] [PubMed]
42. Kanehisa, M.; Furumichi, M.; Tanabe, M.; Sato, Y.; Morishima, K. KEGG: New perspectives on genomes, pathways, diseases and drugs. *Nucleic Acids Res.* **2017**, *45*, D353–D361. [CrossRef]
43. Galperin, M.Y.; Makarova, K.S.; Wolf, Y.I.; Koonin, E.V. Expanded microbial genome coverage and improved protein family annotation in the COG database. *Nucleic Acids Res.* **2015**, *43*, D261–D269. [CrossRef] [PubMed]
44. Vieira, V.V.; Ramos, J.N.; dos Santos, L.S.; Mattos-Guaraldi, A.L. *Corynebacterium*: Molecular Typing and Pathogenesis of *Corynebacterium diphtheriae* and Zoonotic Diphtheria Toxin-Producing *Corynebacterium* Species. In *Molecular Typing in Bacterial Infections, Volume I*; Springer International Publishing: Cham, 2022; pp. 3–35. [CrossRef]

45. Bolt, F.; Cassiday, P.; Tondella, M.L.; DeZoysa, A.; Efstratiou, A.; Sing, A.; Zasada, A.; Bernard, K.; Guiso, N.; Badell, E.; et al. Multilocus Sequence Typing Identifies Evidence for Recombination and Two Distinct Lineages of *Corynebacterium diphtheriae*. *J. Clin. Microbiol.* **2010**, *48*, 4177–4185. [CrossRef] [PubMed]
46. König, C.; Meinel, D.M.; Margos, G.; Konrad, R.; Sing, A. Multilocus Sequence Typing of *Corynebacterium ulcerans* Provides Evidence for Zoonotic Transmission and for Increased Prevalence of Certain Sequence Types among Toxigenic Strains. *J. Clin. Microbiol.* **2014**, *52*, 4318–4324. [CrossRef] [PubMed]
47. Kovanen, S.M.; Kivistö, R.I.; Rossi, M.; Schott, T.; Kärkkäinen, U.-M.; Tuuminen, T.; Uksila, J.; Rautelin, H.; Hanninen, M.L. Multilocus Sequence Typing (MLST) and Whole-Genome MLST of *Campylobacter jejuni* Isolates from Human Infections in Three Districts during a Seasonal Peak in Finland. *J. Clin. Microbiol.* **2014**, *52*, 4147–4154. [CrossRef] [PubMed]
48. Hacker, J.; Carniel, E. Ecological fitness, genomic islands and bacterial pathogenicity. *EMBO Rep.* **2001**, *2*, 376–381. [CrossRef]
49. Ochman, H.; Lawrence, J.G.; Groisman, E.A. Lateral gene transfer and the nature of bacterial innovation. *Nature* **2000**, *405*, 299–304. [CrossRef] [PubMed]
50. Oliveira, P.H.; Touchon, M.; Cury, J.; Rocha, E.P.C. The chromosomal organization of horizontal gene transfer in bacteria. *Nat. Commun.* **2017**, *8*, 841. [CrossRef] [PubMed]
51. Couturier, M.; Bex, F.; Bergquist, P.L.; Maas, W.K. Identification and classification of bacterial plasmids. *Microbiol. Rev.* **1988**, *52*, 375–395. [CrossRef] [PubMed]
52. Shintani, M.; Sanchez, Z.K.; Kimbara, K. Genomics of microbial plasmids: Classification and identification based on replication and transfer systems and host taxonomy. *Front. Microbiol.* **2015**, *6*, 242. [CrossRef] [PubMed]
53. Serwold-Davis, T.M.; Groman, N.; Rabin, M. Transformation of *Corynebacterium diphtheriae*, *Corynebacterium ulcerans*, *Corynebacterium glutamicum*, and *Escherichia coli* with the *C. diphtheriae* plasmid pNG2. *Proc. Natl. Acad. Sci. USA* **1987**, *84*, 4964–4968. [CrossRef] [PubMed]
54. Tauch, A.; Bischoff, N.; Brune, I.; Kalinowski, J. Insights into the genetic organization of the *Corynebacterium diphtheriae* erythromycin resistance plasmid pNG2 deduced from its complete nucleotide sequence. *Plasmid* **2003**, *49*, 63–74. [CrossRef] [PubMed]
55. Hennart, M.; Panunzi, L.G.; Rodrigues, C.; Gaday, Q.; Baines, S.L.; Barros-Pinkelnig, M.; Carmi-Leroy, A.; Dazas, M.; Wehenkel, A.M.; Didelot, X.; et al. Population genomics and antimicrobial resistance in *Corynebacterium diphtheriae*. *Genome Med.* **2020**, *12*, 107. [CrossRef] [PubMed]
56. Fluit, A.C.; Schmitz, F.J. Class 1 Integrrons, Gene Cassettes, Mobility, and Epidemiology. *Eur. J. Clin. Microbiol. Infect. Dis.* **1999**, *18*, 761–770. [CrossRef] [PubMed]
57. Gallardo, A.A.; Toledo, R.A.; González Pasayo, R.A.; Azevedo, V.; Robles, C.; Paolicchi, F.A.; Belchior, S.G.E. *Corynebacterium pseudotuberculosis* biovar ovis: Evaluación de la sensibilidad antibiótica in vitro. *Rev. Argent. De Microbiol.* **2019**, *51*, 334–338. [CrossRef]
58. Arcari, G.; Hennart, M.; Badell, E.; Brisson, S. Multidrug-resistant toxigenic *Corynebacterium diphtheriae* sublineage 453 with two novel resistance genomic islands. *Microb. Genom.* **2023**, *9*, 000923. [CrossRef] [PubMed]
59. Barraud, O.; Badell, E.; Denis, F.; Guiso, N.; Ploy, M.-C. Antimicrobial Drug Resistance in *Corynebacterium diphtheriae* mitis. *Emerg. Infect. Dis.* **2011**, *17*, 2078. [CrossRef] [PubMed]
60. Sekizuka, T.; Yamamoto, A.; Komiya, T.; Kenri, T.; Takeuchi, F.; Shibayama, K.; Takahashi, M.; Kuroda, M.; Iwaki, M. *Corynebacterium ulcerans* 0102 carries the gene encoding diphtheria toxin on a prophage different from the *C. diphtheriae* NCTC 13129 prophage. *BMC Microbiol.* **2012**, *12*, 72. [CrossRef] [PubMed]
61. Yomantas, Y.A.V.; Abalakina, E.G.; Lobanova, J.S.; Mamontov, V.A.; Stoyanova, N.V.; Mashko, S.V. Complete nucleotide sequences and annotations of φ673 and φ674, two newly characterised lytic phages of *Corynebacterium glutamicum* ATCC 13032. *Arch. Virol.* **2018**, *163*, 2565–2568. [CrossRef] [PubMed]
62. Michel, A.; Clermont, O.; Denamur, E.; Tenaillon, O. Bacteriophage PhiX174's Ecological Niche and the Flexibility of Its *Escherichia coli* Lipopolysaccharide Receptor. *Appl. Environ. Microbiol.* **2010**, *76*, 7310–7313. [CrossRef]
63. Leyton-Carcaman, B.; Abanto, M. Beyond to the Stable: Role of the Insertion Sequences as Epidemiological Descriptors in *Corynebacterium striatum*. *Front. Microbiol.* **2022**, *13*, 806576. [CrossRef] [PubMed]
64. Consuegra, J.; Gaffé, J.; Lenski, R.E.; Hindré, T.; Barrick, J.E.; Tenaillon, O.; Schneider, D. Insertion-sequence-mediated mutations both promote and constrain evolvability during a long-term experiment with bacteria. *Nat. Commun.* **2021**, *12*, 980. [CrossRef] [PubMed]
65. Vandecraen, J.; Chandler, M.; Aertsen, A.; Van Houdt, R. The impact of insertion sequences on bacterial genome plasticity and adaptability. *Crit. Rev. Microbiol.* **2017**, *43*, 709–730. [CrossRef] [PubMed]
66. Leyton, B.; Ramos, J.N.; Baio, P.V.P.; Veras, J.F.C.; Souza, C.; Burkovski, A.; Mattos-Guaraldi, A.L.; Vieira, V.V.; Marin, M.A. Treat Me Well or Will Resist: Uptake of Mobile Genetic Elements Determine the Resistome of *Corynebacterium striatum*. *Int. J. Mol. Sci.* **2021**, *22*, 7499. [CrossRef]
67. Xu, Y.; Li, Z. CRISPR-Cas systems: Overview, innovations and applications in human disease research and gene therapy. *Comput. Struct. Biotechnol. J.* **2020**, *18*, 2401–2415. [CrossRef] [PubMed]
68. Karginov, F.V.; Hannon, G.J. The CRISPR System: Small RNA-Guided Defense in Bacteria and Archaea. *Mol. Cell* **2010**, *37*, 7–19. [CrossRef] [PubMed]

69. Hong, K.-W.; Asmah Hani, A.W.; Nurul Aina Murni, C.A.; Pusparani, R.R.; Chong, C.K.; Verasahib, K.; Yusoff, W.N.W.; Noordin, N.M.; Tee, K.K.; Yin, W.F.; et al. Comparative genomic and phylogenetic analysis of a toxigenic clinical isolate of *Corynebacterium diphtheriae* strain B-D-16-78 from Malaysia. *Infect. Genet. Evol.* **2017**, *54*, 263–270. [CrossRef] [PubMed]
70. Viana, M.V.C.; Figueiredo, H.; Ramos, R.; Guimarães, L.C.; Pereira, F.L.; Dorella, F.A.; Selim, S.A.K.; Salaheldean, M.; Silva, A.; Wattam, A.R.; et al. Comparative genomic analysis between *Corynebacterium pseudotuberculosis* strains isolated from buffalo. *PLoS ONE* **2017**, *12*, e0176347. [CrossRef] [PubMed]
71. Burkovski, A. Proteomics of Toxigenic Corynebacteria. *Proteomes* **2023**, *12*, 2. [CrossRef]
72. Museux, K.; Arcari, G.; Rodrigo, G.; Hennart, M.; Badell, E.; Toubiana, J.; Brisson, S. Corynebacteria of the diphtheriae Species Complex in Companion Animals: Clinical and Microbiological Characterization of 64 Cases from France. *Microbiol. Spectr.* **2023**, *11*, e00006-23. [CrossRef] [PubMed]
73. Moreira, L.O.; Mattos-Guaraldi, A.L.; Andrade, A.F.B. Novel lipoarabinomannan-like lipoglycan (CdiLAM) contributes to the adherence of *Corynebacterium diphtheriae* to epithelial cells. *Arch. Microbiol.* **2008**, *190*, 521–530. [CrossRef] [PubMed]
74. Broadway, M.M.; Rogers, E.A.; Chang, C.; Huang, I.-H.; Dwivedi, P.; Yildirim, S.; Schmitt, M.P.; Das, A.; Ton-That, H. Pilus Gene Pool Variation and the Virulence of *Corynebacterium diphtheriae* Clinical Isolates during Infection of a Nematode. *J. Bacteriol.* **2013**, *195*, 3774–3783. [CrossRef] [PubMed]
75. Billington, S.J.; Esmay, P.A.; Songer, J.G.; Jost, B.H. Identification and role in virulence of putative iron acquisition genes from *Corynebacterium pseudotuberculosis*. *FEMS Microbiol. Lett.* **2002**, *208*, 41–45. [CrossRef] [PubMed]
76. Qian, Y.; Lee, J.H.; Holmes, R.K. Identification of a DtxR-Regulated Operon That Is Essential for Siderophore-Dependent Iron Uptake in *Corynebacterium diphtheriae*. *J. Bacteriol.* **2002**, *184*, 4846–4856. [CrossRef] [PubMed]
77. Kunkle, C.A.; Schmitt, M.P. Analysis of a DtxR-Regulated Iron Transport and Siderophore Biosynthesis Gene Cluster in *Corynebacterium diphtheriae*. *J. Bacteriol.* **2005**, *187*, 422–433. [CrossRef] [PubMed]
78. Lyman, L.R.; Peng, E.D.; Schmitt, M.P. *Corynebacterium diphtheriae* Iron-Regulated Surface Protein HbpA Is Involved in the Utilization of the Hemoglobin-Haptoglobin Complex as an Iron Source. *J. Bacteriol.* **2018**, *200*, 1–19. [CrossRef] [PubMed]
79. Dražek, E.S.; Hammack, C.A.; Schmitt, M.P. *Corynebacterium diphtheriae* genes required for acquisition of iron from haemin and haemoglobin are homologous to ABC haemin transporters. *Mol. Microbiol.* **2000**, *36*, 68–84. [CrossRef] [PubMed]
80. Gupta, S.; Bansal, S.; Deb, J.K.; Kundu, B. Interplay between DtxR and nitric oxide reductase activities: A functional genomics approach indicating involvement of homologous protein domains in bacterial pathogenesis. *Int. J. Exp. Pathol.* **2007**, *88*, 377–385. [CrossRef] [PubMed]
81. Yellaboina, S.; Ranjan, S.; Chakhaiyar, P.; Hasnain, S.; Ranjan, A. Prediction of DtxR regulon: Identification of binding sites and operons controlled by Diphtheria toxin repressor in *Corynebacterium diphtheriae*. *BMC Microbiol.* **2004**, *4*, 38. [CrossRef]
82. Allen, C.E.; Schmitt, M.P. Utilization of Host Iron Sources by *Corynebacterium diphtheriae*: Multiple Hemoglobin-Binding Proteins Are Essential for the Use of Iron from the Hemoglobin-Haptoglobin Complex. *J. Bacteriol.* **2015**, *197*, 553–562. [CrossRef] [PubMed]
83. Chapartegui-González, I.; Fernández-Martínez, M.; Rodríguez-Fernández, A.; Rocha, D.J.P.; Aguiar, E.R.G.R.; Pacheco, L.G.C.; Ramos-Vivas, J.; Calvo, J.; Martínez-Martínez, L.; Navas, J. Antimicrobial Susceptibility and Characterization of Resistance Mechanisms of *Corynebacterium urealyticum* Clinical Isolates. *Antibiotics* **2020**, *9*, 404. [CrossRef] [PubMed]
84. Viana, M.V.C.; Galdino, J.H.; Profeta, R.; Oliveira, M.; Tavares, L.; de Castro Soares, S.; Carneiro, P.; Wattam, A.R.; Azevedo, V. Analysis of *Corynebacterium silvaticum* genomes from Portugal reveals a single cluster and a clade suggested to produce diphtheria toxin. *PeerJ* **2023**, *11*, e14895. [CrossRef]
85. Luo, Q.; Luo, H.; Zhang, T.; Liu, X.; Chen, X.; Chen, Q.; Feng, J.; Qu, P.; Chen, C.; Xu, N. *Corynebacterium lipophilum* sp. nov., a lipophilic bacterium isolated from clinical breast specimens and emended description of the species *Corynebacterium pilbarensis*. *Antonie Van Leeuwenhoek* **2023**, *116*, 1091–1101. [CrossRef] [PubMed]
86. Ishikawa, J.; Chiba, K.; Kurita, H.; Satoh, H. Contribution of rpoB2 RNA polymerase beta subunit gene to rifampin resistance in *Nocardia* species. *Antimicrob. Agents Chemother.* **2006**, *50*, 1342–1346. [CrossRef] [PubMed]
87. Bosi, E.; Fani, R.; Fondi, M. Defining Orthologs and Pan-genome Size Metrics. *Methods Mol. Biol.* **2015**, *1231*, 191–202. [CrossRef] [PubMed]
88. Costa, S.S.; Guimarães, L.C.; Silva, A.; Soares, S.C.; Baraúna, R.A. First Steps in the Analysis of Prokaryotic Pan-Genomes. *Bioinform. Biol. Insights* **2020**, *14*, 11779322093806. [CrossRef] [PubMed]
89. Viana, M.V.C.; Profeta, R.; da Silva, A.L.; Hurtado, R.; Cerqueira, J.C.; Ribeiro, B.F.S.; Almeida, M.O.; Morais-Rodrigues, F.; Soares, S.C.; Oliveira, M.; et al. Taxonomic classification of strain PO100/5 shows a broader geographic distribution and genetic markers of the recently described *Corynebacterium silvaticum*. *PLoS ONE* **2020**, *15*, e0244210. [CrossRef] [PubMed]
90. Soares, S.C.; Silva, A.; Trost, E.; Blom, J.; Ramos, R.; Carneiro, A.; Ali, A.; Santos, A.R.; Pinto, A.C.; Diniz, C.; et al. The Pan-Genome of the Animal Pathogen *Corynebacterium pseudotuberculosis* Reveals Differences in Genome Plasticity between the Biovar ovis and equi Strains. *PLoS ONE* **2013**, *8*, e53818. [CrossRef] [PubMed]
91. Trost, E.; Blom, J.; de Castro Soares, S.; Huang, I.-H.; Al-Dilaimi, A.; Schröder, J.; Jaenicke, S.; Dorella, F.A.; Rocha, F.S.; Miyoshi, A.; et al. Pan-genomic Study of *Corynebacterium diphtheriae* That Provides Insights into the Genomic Diversity of Pathogenic Isolates from Cases of Classical Diphtheria, Endocarditis, and Pneumonia. *J. Bacteriol.* **2012**, *194*, 3199–3215. [CrossRef] [PubMed]

92. Ott, L.; Möller, J.; Burkovski, A. Interactions between the Re-Emerging Pathogen *Corynebacterium diphtheriae* and Host Cells. *Int. J. Mol. Sci.* **2022**, *23*, 3298. [[CrossRef](#)] [[PubMed](#)]
93. Sangal, V.; Burkovski, A.; Hunt, A.C.; Edwards, B.; Blom, J.; Hoskisson, P.A. A lack of genetic basis for biovar differentiation in clinically important *Corynebacterium diphtheriae* from whole genome sequencing. *Infect. Genet. Evol.* **2014**, *21*, 54–57. [[CrossRef](#)] [[PubMed](#)]

Disclaimer/Publisher’s Note: The statements, opinions and data contained in all publications are solely those of the individual author(s) and contributor(s) and not of MDPI and/or the editor(s). MDPI and/or the editor(s) disclaim responsibility for any injury to people or property resulting from any ideas, methods, instructions or products referred to in the content.